

Universal Code

A Mohamed Wahid

Civil Engineer, 21, First Floor, Third Main Road, Vasanth Nagar, Bangalore – 560052, India

Email: [S1623jn26\[at\]yahoo.fr](mailto:S1623jn26[at]yahoo.fr)

Abstract: *Conventional personal identification methods (ID, password, authorization certificate, etc.) entail various issues, including forgery or loss. Technological advances and the diffusion across industries have enhanced convenience; however, privacy risks due to security attacks are increasing. Hence, personal identification based on biometrics such as the face, iris, fingerprints, and veins has been used widely. However, biometric information including faces and fingerprints is difficult to apply in industries requiring high-level security, owing to tampering or forgery risks and recognition errors. This paper proposes a personal identification technique based on Coccyx with an Artificial Intelligence.*

Keywords: Universal Code, Personal identification; Convolutional Neural network; Ensemble approach

1. Introduction

The rapid advancement of artificial intelligence (AI) has achieved significant progress and, thereby, has gained substantial attention worldwide. Since the emergence of deep learning (a core technology of AI), the applications of AI technology have been expanded to various fields for increased convenience in daily human life. In addition, it has improved the quality of life through its applications in the medical, agricultural, financial, and autonomous vehicle fields. Notwithstanding the positive influences of technology advancement and diffusion, certain risks are imposed on humans as intelligent cyber-attacks increase. An array of personal authentication technologies has been studied to defend against similar threats.

Personal information has been protected using passwords or OTPs. However, recently, technologies using biometrics for protecting personal information have been employed increasingly to address the risk of loss or theft. These technologies can conveniently and safely manage personal information as well as verify the identity of users. As a consequence, personal authentication technology using biometric information such as voice, gender, face, and behaviour is being actively developed and used. Seven characteristics are required for biometric recognition. Fundamental characteristics such as universality (indicates whether every individual has the information), uniqueness (indicates the distinctiveness of each individual's information), permanence (indicates whether the information remains unaltered over time and is modifiable), and collectability (indicates whether the biometric can be acquired conveniently using sensors) are required. The following characteristics are required for trusting and

Using biometrics: accuracy including the speed and precision of receiving and processing information, accessibility that does not induce reluctance to biometric measurement, and safety against inappropriate use to achieve deception security.

Compared with simple serpentine patterns, fractal serpentine designs gained larger areal filling factors and supported various deformation modes, including biaxial and radial



Figure 1: Future Human with Universal Code

deformation Stretch ability could be enhanced as the hierarchy of self-similar

serpentine increased. Fractal-enabled, highly stretchable epidermal electronics have been used for joule heating, Temperature sensing, and ECG measurement. Although serpentine provide sufficient stretch ability, their mechanical properties do not

precisely match the nonlinear behaviour of bio-tissues. As a result, a 2D triangular lattice with horseshoe serpentine has been designed, the stress/strain response of which can be tailored to fully overlap with that of human skin.

1.1 AI Data Collection & Communication Systems

Microfluidics is both the science which studies the behaviour of fluids through micro-channels, and the technology of manufacturing microminiaturized devices containing chambers and tunnels through which fluids flow or is confined.

Microfluidics deal with very small volumes of fluids, down to femtoliters (fL) which is a quadrillionth of a liter. Fluids behave very differently on the micrometric scale than they do in everyday life: these unique features are the key for new scientific experiments and innovations.

The key concept related to microfluidics is to integrate in a simple micro-sized system operations that commonly solicit a whole laboratory.

Volume 13 Issue 4, April 2024

Fully Refereed | Open Access | Double Blind Peer Reviewed Journal

www.ijsr.net

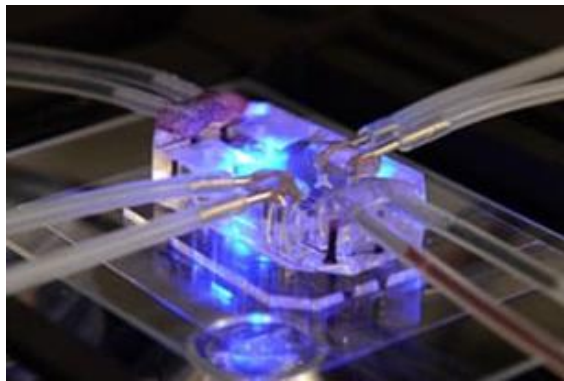


Figure 2: Organs on chips are 3D cell culture micro devices

A microfluidic chip is a pattern of micro channels, moulded or engraved. This network of micro channels incorporated into the microfluidic chip is linked to the macro-environment by several holes of different dimensions hollowed out through the chip. It is through these pathways that fluids are injected into and evacuated from the microfluidic chip. Fluids are directed, mixed, separated or manipulated to attain multiplexing, automation, and high-throughput systems. The micro channels network design must be precisely elaborated to achieve the desired features (lab-on-a-chip, detection of pathogens, electrophoresis, DNA analysis etc.).

To accurately manage fluids inside the micro channels, specific systems are required. These elements can either be found embedded inside the microfluidic chip, such as Quake valves, or outside of it, like in the case of pressure controllers.

Microfluidic devices exploit the physical and chemical properties of liquids and gases at a micro scale. Microfluidic devices offer several benefits over conventionally sized systems. Microfluidics allows the analysis and use of less volume of samples, chemicals and reagents reducing the global fees of applications. Many operations can be executed at the same time thanks to their compact size, shortening the time of experiment. They also offer an excellent data quality and substantial parameter control which allows process automation while preserving the performances. They have the capacity to both process and analyse samples with minor sample handling. The microfluidic chip is elaborated so that the incorporated automation allows the user to generate multi-step

Functionalities. The microsystems execute functions that extend from detecting toxins to analysing DNA

Sequences or creating inkjet printing devices. To learn more about microfluidics applications, visit our dedicated review here.

Microfluidics has diverse assets: faster reaction time enhanced analytical sensitivity, enhanced temperature control, portability, easier automation and parallelization, integration of lab routines in one device (lab-on-a-chip). It is cheap as it does not involve the use of various costly equipment. To have a look at the many technologies in the field, you can check out the only distributor specialized in microfluidics, Darwin Microfluidics.

Today, microfluidics provides efficient tools for multiple research areas, and more specifically for biological analysis:

- Whole biological process integrated and simplified for the end-users
- High-throughput, multiplexed and highly paralleled assays
- Faster analyses due to the shorter reactions and/or separation times
- Portable devices for point-of-care applications
- Low reagent consumptions
- Global cost reduction per analysis
- Accurate measurement, microfluidics allowing to increase the measurement resolution in given applications

Soft lithography for microfluidics

In microfluidics, soft lithography is a diverse set of techniques that use a soft elastomer material (most of the time PDMS) to transfer patterns to a substrate material.

The basic process consists in building elastomeric micro channels. These micro channels are designed in a specific program and then printed onto a high-resolution transparency mask or remodelled into a conventional chrome mask to produce a master which will serve as a mould for the soft material.

Soft lithography presents various advantages over other forms of lithography, among which we can find its low cost and easy fabrication process; its rapidity, its tolerance over a wide variety of materials. In addition, soft lithography allows creating precisely delimited and manageable surface chemistries. It is also compatible with numerous applications that include cell biology, microfluidics, lab-on-a-chip or MEMS.

Soft lithography can be divided into 3 different major subcategories which are replica moulding, micro contact printing and embossing.

Replica molding in microfluidics

Replica moulding in microfluidics allows transferring a pattern from a rigid or elastomeric mould called a master into another material, by way of a liquid polymeric mixture which starts to solidify when it gets in contact with the master.

A micro scale pattern is generated with computer-assisted design software before being transferred on a photo mask. A thin uniform film called photoresist is spin-coated on a silicon wafer, which is then covered with the photo mask. Liquid polymeric mixture is poured onto the silicon master before being baked or exposed to UV light. Thanks to heat, the replica solidifies, leaving the micro scale pattern etched into the photoresist. The desired feature it is then peeled away from the master mould and sealed.

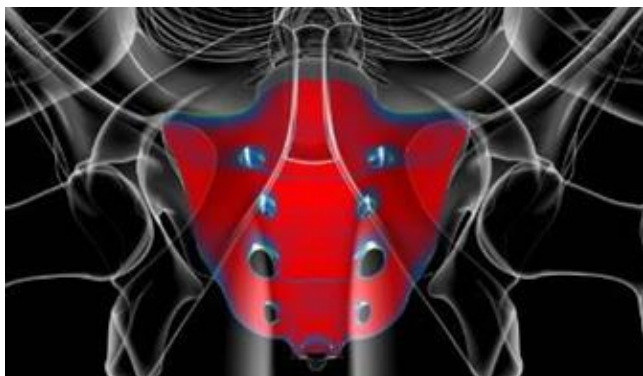


Figure 3: Soft lithography for microfluidics

Replica moulding can be repeated multiple times and allows patterning a wide range of materials. This chip has the potential to serve as a human identifier. Since until Coccyx annihilate this chip will be alive.

2. Heading

2.1 Artificial Intelligence Utilizing Living Human Coccyx achieves self-Recognition.

Humans are still necessary for decision-making, creativity, and empathy. AI can assist humans in making decisions by providing data-driven insights; it can be replace human judgment. At Inclusion Cloud, we specialize in providing technological solutions to businesses that enable human-AI collaboration.

2.2 Artificial Intelligence Utilizing Living Human Coccyx achieves self-Recognition.

Systems Biology is a field of biology that aims to understand biological systems holistically and interactively, including their structures, functions, and interactions. The complexity of biological systems makes it difficult to understand their behaviour and predict their responses to perturbations or interventions. To overcome this challenge, researchers need to integrate and analyse vast amounts of heterogeneous data from various sources, such as genomics, transcriptomics, proteomics, and metabolomics, to build comprehensive models of biological systems. These models can help identify new drug targets, design personalized therapies, and develop strategies to prevent or treat diseases. However, the integration and analysis of large and complex data sets are beyond the capabilities of human experts, and this is where artificial intelligence (AI) comes in.

Multi-omics data is the collection of multiple types of molecular data from a single biological sample. Such data can include genomics (the study of the DNA sequence), transcriptomics (the analysis of gene expression), proteomics (the study of proteins), metabolomics (the study of tiny molecules), and other types of molecular data. Integrating multiple omics data sources is a powerful approach to understanding complex biological processes and disease mechanisms. Such integration has different challenges, such as integrating copy number variation (CNV) and copy number alteration (CNA) data into multi-omics analyses. One challenge is CNV and CNA data heterogeneity across different

technologies and platforms. Different methods for detecting CNVs and CNAs can lead to differences in the types and frequency of aberrations detected, making it difficult to compare and integrate data across studies. Another challenge is interpreting CNV and CNA data within the context of other omics data. While CNVs and CNAs can significantly impact gene expression and protein activity, their effects can be complex, nonlinear, and vary depending on the specific biological context.

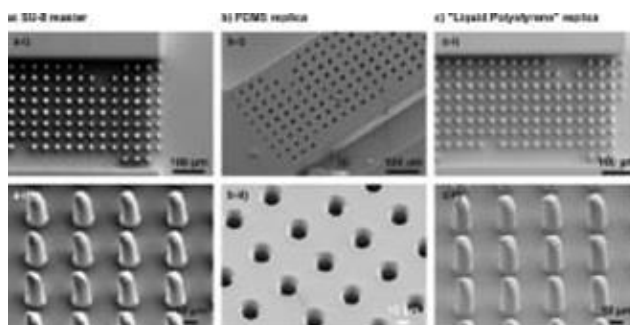


Figure 4: Microfluidics Chip Inject in to Coccyx

Another area in Systems Biology needs AI to develop models that simulate the behaviour of biological systems. AI-based techniques, such as artificial neural networks and genetic algorithms, can be used to generate models that accurately capture the dynamics of biological systems and can be used to make predictions about the behaviour of these systems under different conditions. AI can also help in drug discovery and development. By applying machine learning algorithms to large datasets of molecular structures and their associated biological activities, researchers can identify potential drug candidates more quickly and accurately than with traditional methods (Gupta et al., 2021). Here, AI can model protein–ligand interactions. AI-based methods can predict the binding affinity of a ligand to a protein and the location and orientation of the ligand within the protein's active site.



Figure 5: Flexible Microfluidics Chip inside Coccyx

Structural systems biology is an interdisciplinary field that combines systems biology and structural biology to study biological systems at a molecular level. The area aims to comprehensively understand how biological molecules interact and function within cells, tissues, and organisms. AI has increasingly become an inherent part of structural systems biology to analyse large and complex datasets and model biological systems' behaviour. AI helps structural systems biology in the analysis of protein–protein interaction networks. These networks can be analysed using graph theory and other mathematical approaches, revealing essential features such as hubs and modules (Kantelis et al., 2022). AI-based methods

predict the functions of uncharacterized proteins based on their position in the network and identify potential drug targets based on the network topology (Pan et al., 2023).

In summary, AI can develop models that simulate the behaviour of biological systems at a molecular level. These models can be used to predict the effects of genetic mutations, environmental factors, and drugs on the behaviour of biological systems. AI-based methods can optimize the parameters of these models and identify the key features that drive the system's behaviour. Overall, using AI in Systems biology can provide new insights into the structure–function relationships of biological molecules and identify new targets for drug development. Thus, AI has tremendous potential to help researchers understand and analyse complex biological systems and may lead to new insights and discoveries in biology, medicine, and biotechnology.

2.3 Deep space Network – communication between space and human body.

Communicating to and from space is a challenging endeavour. Fortunately, NASA has the experience and expertise to get space data to the ground. NASA's Space Communications and Navigation (Scan) program enables this data exchange, whether it's with astronauts aboard the International Space Station, rovers on Mars, or the Artemis missions to the Moon. Let's look at some of the challenges of space communications alongside the technologies and capabilities NASA uses to overcome them.

1) The Basics

At its simplest, space communications relies on two things: a transmitter and a receiver. A transmitter encodes a message onto electromagnetic waves through modulation, which changes properties of the wave to represent the data. These waves flow through space toward the receiver. The receiver collects the electromagnetic waves and demodulates them, decoding the sender's message. Consider a Wi-Fi router and networked devices around the home. Each device receives signals from the router, which transmits data from the internet. At its heart, the complex task of communicating with space resembles wireless communications in the home – only on an enormous scale and at incredible distances.

2) Ground Networks

Communicating from space involves more than pointing a spacecraft's antenna at the Earth. NASA has an extensive network of antennas around the globe — over all seven continents — to receive transmissions from spacecraft. Network engineers carefully plan communications between ground stations and missions, ensuring that antennas are ready to receive data as spacecraft pass overhead. Ground station antennas range from the small very high frequency antennas that provide backup communications to the space station to a massive, 230-foot antenna that can communicate with far-off missions like the Voyager spacecraft, over 11 billion miles away.

3) Space Relays

In addition to direct-to-Earth communications, many NASA missions rely on relay satellites in order to get their data to the ground. For example, the space station communicates through

Tracking and Data Relay Satellites (TDRS), which transmit data to ground stations in New Mexico and Guam. The recently launched Mars 2020 Perseverance rover will send data through orbiteers around Mars, which forward the data to Earth. Relays offer unique advantages in terms of communications availability. For example, the placement of TDRS at three different regions above Earth offers global coverage and near-continuous communications between low-Earth orbit missions and the ground. Rather than waiting to pass over a ground station, TDRS users can relay data 24 hours a day, seven days a week.

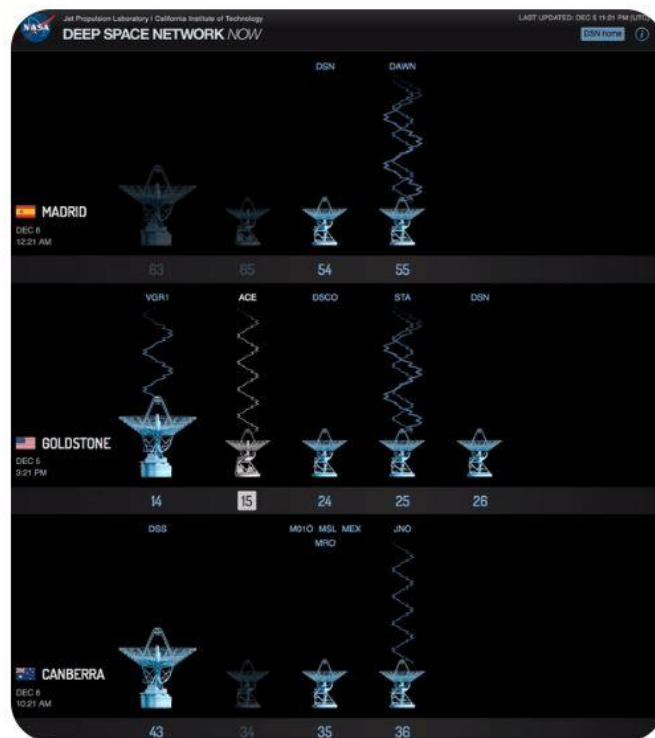


Figure 6: The lines represent information passing between the spacecraft and the DSN antennas.

4) Bandwidth

NASA encodes data on various bands of electromagnetic frequencies. These bandwidths — range of frequencies — have different capabilities. Higher bandwidths can carry more data per second, allowing spacecraft to downlink data more quickly. Currently, NASA relies primarily on radio waves for communications, but the agency is developing ways to communicate with infrared lasers. This type of transmission — dubbed optical communications — will offer missions higher data rates than ever before. NASA's Laser Communications Relay Demonstration (LCRD) will showcase the benefits of optical communications. The mission will relay data between ground stations in California and Hawaii over optical links, testing their capabilities. NASA will also furnish the space station with an optical terminal that can relay data to the ground via LCRD.

5) Data Rates

Higher bandwidths can mean higher data rates for missions. Apollo radios sent grainy black and white video from the Moon. An upcoming optical terminal on the Artemis II mission will send 4K, ultra-high definition video from lunar orbit. But bandwidth isn't the only constraint on data rates. Other factors that can affect data rates include the distance between the

transmitter and receiver, the size of the antennas or optical terminals they use, and the power available on either end. NASA communications engineers must balance these variables in order to maximize data rates.

6) Latency

Communications don't occur instantaneously. They're bound by a universal speed limit: the speed of light, about 186,000 miles per second. For spacecraft close to Earth, this time delay — or communications latency — is almost negligible. However, farther from Earth, latency can become a challenge. At Mars' closest approach — about 35 million miles away — the delay is about four minutes. When the planets are at their greatest distance — about 250 million miles away — the delay is around 24 minutes. This means that astronauts would need to wait between four and 24 minutes for their messages to reach mission control, and another four to 24 minutes to receive a response.

As NASA prepares to send humans to the Red Planet, communications engineers are developing ways for astronauts to stay connected with Earth while recognizing delays will be a part of the conversation.

7) Interference

As communications transmissions travel over long distances or through the atmosphere, the quality of their data can deteriorate, garbling the message. Radiation from other missions, the Sun, or other celestial bodies can also interfere with the quality of transmissions. To make sure that mission operations centres receive accurate data, NASA uses methods of error detection and correction. Methods of error correction include computer algorithms that interpret noisy transmissions as usable data.

While Hollywood dreams up stories that connect people across the galaxy with ease, NASA engineers endeavour to turn those dreams into reality. NASA is developing technologies and capabilities that address the real-world challenges of space communications, while empowering science and exploration missions with robust communications services.

2.4 Radio wave into Human body.

Damaging effect to the human body by radio waves will result if the waves are intense enough to heat up the body. The extreme example is what happens to meat put in a microwave oven.

If a person's body is immersed in a strong radio wave field the electrons and ions in the body try to oscillate in unison with the radio waves. This means energy is extracted from the radio wave and converted to tiny oscillatory motions of electrically-charged components of the body. The more the motion, the higher the body temperature.

In the Soviet Union, regulations require that workers not be exposed to radio wave radiation in excess of 10 microwatts per square centimetre. One hundred times this radiation level (i.e., 1 mill watt per square centimetre) will create slight temperature increase in humans, the rise being about the same as results from normal light physical activity. Prolonged exposure to this intensity of radio wave radiation probably causes permanent

damage. Exposure to 10 to 100 mill watts definitely causes damage to the eyes; it cooks the eye lens enough to cause cataracts.

Scientists and the government agencies charged with protecting human health in Western countries are unwilling, so far, to agree with claims by their eastern European and Soviet counterparts that very low microwave levels (10 microwatt to 1 mill watt) are dangerous. However, they admit that it is an open question.

One reason the question is unanswered is that the energy absorbed by a human from radio waves depends upon the relationship between the size of the human and the frequency of the radio waves. Just as a TV antenna of the right length and orientation figures up the best signal (the most energy) from a transmitted wave, so it is with a human being. It appears that the cranial cavity of a mammal will resonate at specific radio frequencies determined by the size of the brain cavity. At these resonant frequencies the human head will absorb vastly more radio wave energy than it will at other nearby frequencies.

An adult's head will resonate at a frequency between 350 and 400 MHz (megahertz). Being smaller, a child's head will resonate at a higher frequency, somewhere between 600 and 850 MHz since each individual may have his or her own resonant frequency, a particular frequency radiowave might affect one person more than another. Consequently, testing on humans—even if people are willing to let this happen—can be rather complicated.

Aside from the question of permanent damage by absorption of too much radio wave energy, there is the issue of how much radiation it takes to temporarily modify human behaviour or mental ability. It is suspected that a microwave signal modulated (i.e., pulsed) at the frequencies where human brainwaves operate (1 to 20 Hz) may affect mental processes, even if the radiation is too weak to create substantial heating of the brain.

Quite obviously it is a complicated issue to determine the effects of radio waves upon humans and other animals. Just knowing the strength of the radio signal a person is immersed in is not enough? Critically important may be the frequency match between the signal and the person's body and whether or not the signal is modulated at a frequency that could match up to a person's brainwave pattern.

Complicating matters even further is the finding that mammals can be made to "hear" pulses of radio wave emission. Pulses at frequencies within a mammal's hearing range can cause periodic healings of the head. These create pressure pulses in the ear that are interpreted as sound. Further, some studies have indicated radio wave effects upon cell processes that could affect the nervous system, the cardiovascular system and immunity to disease. The effects are not necessarily all bad: certain cancers are being successfully treated with radio waves, and the future of even greater success looks bright.

2.5 Analog Signal into Human body.

In analog signal, the physical quantities such as current or voltage varies continuously with time. These signals get stored

in the form of wave signal. It also has low impedance. Example- Sinusoidal wave, triangular wave, etc.

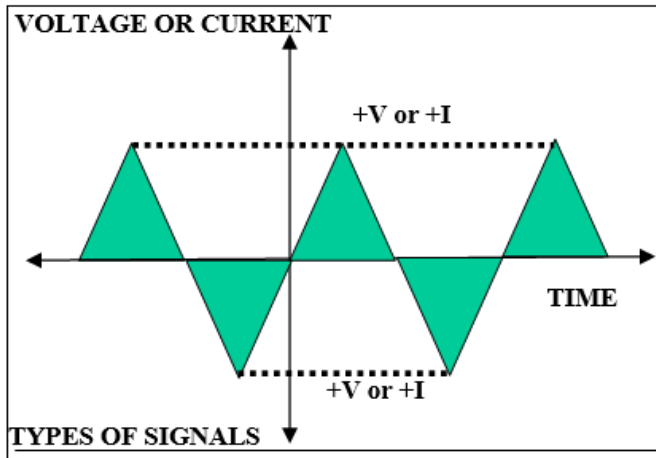


Figure 7: Analog Signal

2.6 Digital Signal into Human body

In digital signal, the physical quantities such as current or voltage can have only one of the two possible values at a time, i.e., digital signal have only levels, either zero or some maximum finite value of current or voltage. These signals get stored in the form of binary bit. It is having high impedance which may reach to 100 mega ohms

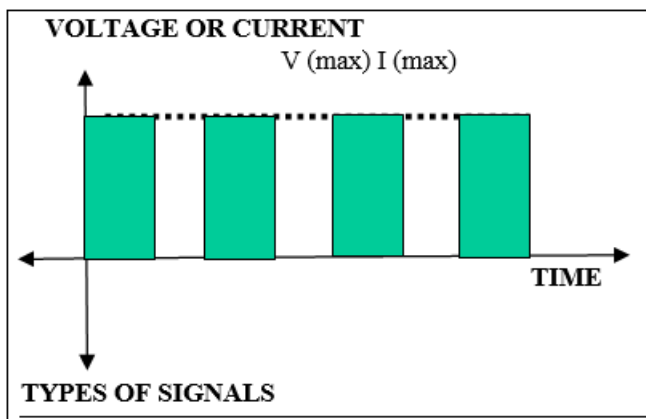


Figure 8: Digital Signal

2.7 Discrete Time Signal into Human body

In discrete-time signal at each point of time, signal will have distinct or discontinuous values. These types of signals can be analysed using techniques like discrete Fourier transformations or z-transformations. It requires less space than continuous-time signal as they are represented by some specific set of numbers. Discrete-time signal has finite bandwidth.

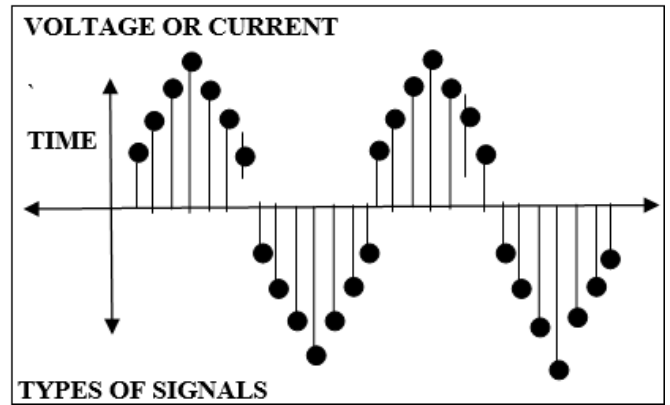


Figure 9: Discrete Time Signal

2.8 Advantages of Signals

Some of the main advantages of signal are given below:

Signals are used in transfer of information as they travel with speed of light, and thus facilitate faster communication. Signals are easily convertible to analog to digital form which facilitates working on many devices via signal. Signals are used in calibrating various instruments which helps in producing accurate and precise results.

2.9 Disadvantages of Signals

Some of the demerits of signal are listed below:

Resulting in misuse of sensitive information.

Signal which is to be delivered to receiver may be attenuated, which results in loss of information which was present in signal. Signals are prone to error during propagation by another signal or by any external factor, thus it results in degradation of quality and reliability of information.

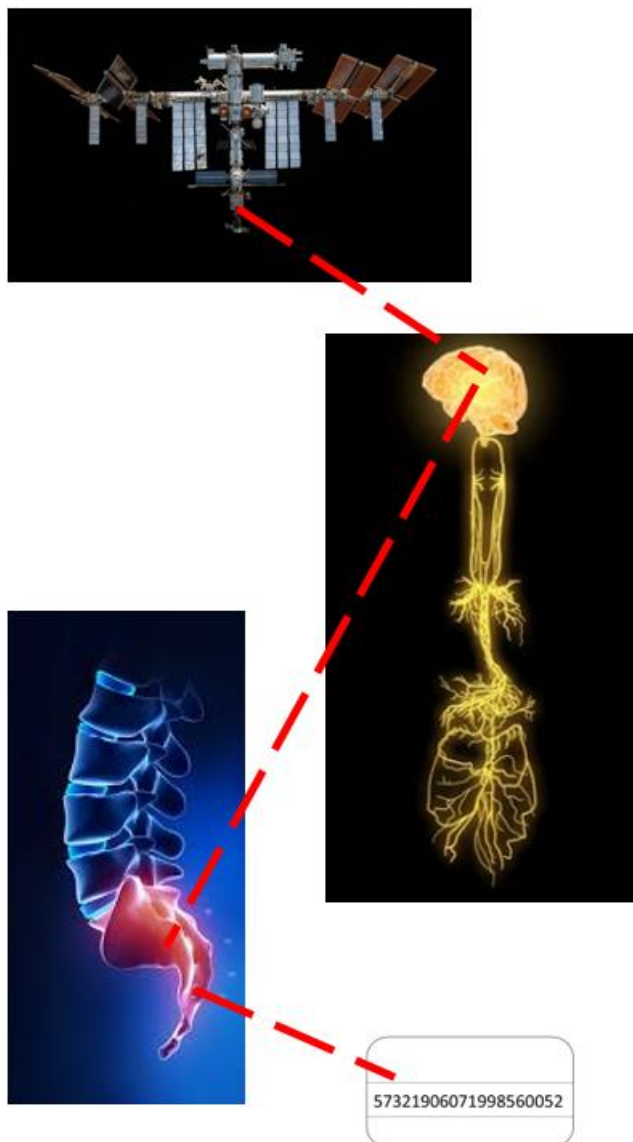


Figure 10: Signal connectivity between Brain, Coccyx IMFC, Universal Code and Space shuttle

3. Signal Transmission VS. COCCYX

Implantable medical devices, such as neurostimulators, need to be wirelessly controlled from outside the body. Many of these devices use high-frequency signals in the 400 MHz, 900 MHz, and 2.45 GHz bands to communicate with external devices. However, high-frequency bands can suffer from signal attenuation in biological tissues and from electromagnetic interference with surrounding devices. In contrast, human body communication (HBC) uses relatively low frequencies in the 3–30 MHz band, which can alleviate signal attenuation and prevent emissions outside the body during communication. In this study, we investigated the use of HBC for implantable medical devices in the abdomen using electromagnetic field simulations. The results showed that the transmission between the transmitter inside the body and the receiver outside the body was adequate for stable communication. However, when the receiver was detached from the skin surface, the transmission characteristics rapidly decreased. Moreover, when the receiver and skin were separated by 1 mm, the transmission degraded by 34 dB, indicating that electromagnetic interference between the implanted

transmitter and surrounding devices (including other medical devices) is rare. Finally, we evaluated the proposed system from the perspective of medical electromagnetic compatibility and human safety. The simulation results demonstrated that the radiated emissions and human exposure of the HBC system meet international standards.

3.1 History of Implantable Microchips

Carried out by the British scientist, Kevin Warwick. His implant was utilized to activate lights, unlock doors, and produce verbal output inside a structure. The implant was removed after nine days and is now kept in the London Science Museum. Further research in this field was carried forward by Nokia, Phillips and Sony in 2004 by implementation and promotion of NFC technology to ensure interoperability between devices and services. In 2018, VivoKey Technologies created the first human implantable NFC transponders that are cryptographically secure. Further advancement in the field happened in 2019 when MIT received funding from the Bill & Melinda Gates Foundation to create a vaccine and an invisible micro needle patch that can store digital medical information. More development happened when, Elon Musk, the CEO of Neuralink, unveiled a company-directed live video podcast on August 28, 2020, featuring a pig named Gertrude with a coin-sized computer chip in her brain to show off his bold aspirations to develop a functional brain-to-machine interface. Further development in the regards to implantable microchip continues. In fact there are many individuals who are using implantable microchips as well.



Figure 11: Intelligent Micro Fluid Chip inside Coccyx

3.2 Advantages of Implantable IMFC (Intelligent Micro Fluid Chip)

The widespread use of IMFC technology has the potential to fundamentally alter the way that modern healthcare is delivered. The quality of life for patient populations will improve, therapeutic procedures will change, and wasteful costs amounting to billions of dollars will be saved. The position of microchips in medicine nowadays can be learned via a review of noteworthy patents, recent microchip developments, and clinically applicable uses, as well as by inspiring new research fields. There are many advantages of Implantable microchips. Few of these are mentioned below:

Implantable microchips can be used as a transdermal drug delivery system in which we can alter the rate at which the drug gets delivered to the patient. Drugs with dose administration methods that would normally be difficult or undesirable might be administered passively. Treatments for conditions requiring

dose titrations, such as diabetes and hypertension, could be transformed to produce automated therapy regimens that are both safer and more effective. This controlled-release technique, when utilised with implants, will lessen the possibility of foreign body reactions and rejection, which will lessen the possibility of inflammation and pain and enable the body to recover from surgery more quickly.

Artificial glands could be made using microchip technology. Regulation of hormones in the body linked to malfunctioning glands may help control existing illness conditions and delay the advent of additional hormone-induced ailments.

Treatments for conditions that typically have a reduced rate of compliance (mental illnesses, some cancer therapies, long-term antibiotics, etc.) or misuse potential will benefit from the adoption of microchip delivery systems.

Implantable microchips are also used for digital identity. Using IMFC, implantable microchips provide the individuals with a unique identity. This can be used to access a lot of things ranging from medical records to bank accounts.

Other uses are in the form of address book, green card, travel cards, credit cards, as well as for crypto transactions, Passport, Student ID card, Staff ID card, Visa, Driving licence, Adhaar Card and any human identification of Bio metric also finger prints.

It contains one ID for entire process. Anyone having this ID and work permit, he/she can fly anywhere without any restriction.

3.3 Simulation setup

An electromagnetic field simulation model was used to study the communication between an implantable abdominal medical device and a controller on the skin surface. The dimensions of the abdominal model were determined based on the average shape of a Japanese adult male. The model was composed of skin, fat, and muscle layers, and we determined the electrical properties of each tissue layer referencing our previously developed electromagnetic phantoms, which can be used at 10–30 MHz

Lists the relative permittivity and conductivity of each layer. Using the electrical properties of phantoms will facilitate a comparison between future simulations and experimental results. The overall dimensions of the abdominal model were $260 \times 210 \times 190$ mm, and the thicknesses of the skin, fat, and muscle layers were 2, 6, and 182 mm, respectively. To determine the thickness of each tissue layer, we considered the thickness range of each abdominal tissue.

The thickness ranges reasonably compared with those in conventional studies of multi-layer abdominal tissue Phantoms.

The implantable device (sized $48 \times 48 \times 10$ mm) was fixed to the fascia within 2 cm of the skin surface, reproducing the situation of actual implantable stimulators.

Agree space was created in the muscle layer to accommodate the device housing.

In this study, the implantable device was the transmitter (TX) and the controller outside the body was the receiver (RX). An 8×24 mm

Two-electrode structure, commonly used in wearable HBC systems,



Figure 12: Intelligent Micro Fluid Chip design

Was used as the communication electrode, which was placed in the centre of the model. The TX electrode was placed in contact with the lower part of the fat layer, while the RX electrode was placed on the surface of the skin layer. From a human safety perspective, implantable electrodes should be formed from biocompatible materials, such as titanium.

We confirmed that the electrical conductivity of titanium ($0.6-2.0 \times 10$)

Electrodes do not affect signal transmission in terms of an electrode material. Therefore, all electrodes were constructed from perfect electrical conductors. The impedance of the TX electrode at the feeding point and the receiving load of the RX were both 50Ω . When selecting the signal frequency (10 MHz), we consulted previous studies

And considered the 13.56-MHz industry–science–medical band.

The finite-difference time-domain method-based electromagnetic field simulator XFDTD (Remcom Inc., PA, and USA) was used to calculate the transmission characteristics, electric field distributions, and input impedance of the electrodes. The computing space of the simulation was represented by non-uniform grids, with grid sizes of 1 mm around the electrodes and 2 mm at the edge of the computing space. The distance between the model edge and the absorbing boundary was 20 cells thick. The absorbing boundary was a perfectly matched layer composed of seven sub layers. The time step of the calculation was 1.926 ps.

4. Universal Code Overview

The rapid advancement of artificial intelligence (AI) has achieved significant progress and, thereby, has gained substantial attention worldwide. Since the emergence of deep learning (a core technology of AI), the applications of AI technology have been expanded

To various fields for increased convenience in daily human life. In addition, it has improved the quality of life through its applications in the medical, agricultural, financial, and autonomous vehicle fields. Notwithstanding the positive influences of technology advancement and diffusion, certain risks are imposed on humans as intelligent cyber-attacks increase. An array of personal authentication technologies has been studied to defend against similar threats. Personal information has been protected using passwords or OTPs. However, recently, technologies using biometrics for protecting personal information have been employed increasingly to address the risk of loss or theft. These technologies can conveniently and safely manage personal information as well as verify the identity of users. As a consequence, Personal authentication technology using biometric information such as voice, gender, face, and behaviour is being actively developed and used. Seven characteristics are required for biometric recognition. Fundamental characteristics such as universality (indicates whether every individual has the information), uniqueness (indicates the distinctiveness of each individual's information), permanence (indicates whether the information remains unaltered over time and is UN modifiable), and collectability (indicates whether the biometric can be acquired conveniently using sensors) are required. The following characteristics are required for trusting and using biometrics: accuracy including the speed and precision Of receiving and processing information, accessibility that does not induce reluctance to biometric measurement, and safety against inappropriate use to achieve deception security. Biometric recognition involves behavioural characteristics such as voice, gait, electrocardiogram (ECG), and brain waves as well as physical characteristics including the face, fingerprints, and the iris. The advantage of face recognition is that facial features can be identified rapidly and conveniently. However, recognition may be ineffective when facial expressions or lighting vary. Fingerprint recognition is used widely. Here, application sensors are used to capture fingerprint images. Although fingerprint recognition is simple, it is sensitive to skin wounds and impurities and can be forged or tampered with. However, recently, face or fingerprint recognition has been difficult to implement in public places during the pandemic because of the need for everyone to wear facemasks. Although voice recognition is a convenient and safe technology because it uses features extracted from voices, recognition may be difficult because of the use of a recorded file or the presence of noise. Gait recognition is a technology that involves an analysis of a user's gait characteristics, which is considerably influenced by the surrounding environment. The application of biometric information expressed outside the body is encountering severe problems owing to personal damage caused by user recognition error as well as forgery and tampering. Accordingly, research is being actively conducted on personal identification using internal signals of the human body, such as electroencephalogram (EEG), electromyogram (EMG), and ECG. EEG is a test that measures an electrical signal at the scalp. It is utilized in brain-computer interfaces (BCIs) and medical diagnosis. However, humans are reluctant to attach sensors to their head for signal measurement. Furthermore, signals may be distorted as these pass through the cranial bone. EMG records the signals generated by muscles. It is utilized in motion recognition, medical diagnosis, and rehabilitation treatment. However, signals must be set for each motion.

Moreover, the sensors need to be accurately attached to the muscle position. ECG shows the electrical signals of the heart's rhythm through a micro-current, which consists of the P wave (atrial depolarization), QRS complex wave (ventricular depolarization), and T wave (ventricular repolarization). The ECG signal is unique to each individual and depends on the size and position of the heart, gender, and age. The 12-lead ECG involves the measurement of signals from both the wrists. It is utilized for medical diagnosis as well as personal identification. Because ECG measures a signal generated inside the human body, it is difficult to replicate or tamper and is unaffected by environmental transformations. Furthermore, all living humans have these signals. Identification based on physiological characteristics such as EEG, EMG, and ECG has been researched extensively for security methods based on personal signals because of its various advantages. However, this study conducted personal identification using ECG, which displays all the seven characteristics of biometric recognition. In recent years, research on personal identification using deep learning has been Conducted actively. The first study on user recognition using ECG was conducted by Biel. It can be classified into handcrafted and non-handcrafted fiducially-based methods. Handcrafted feature extraction methods are based on the characteristics of ECG, namely, the ECG signal amplitude, time interval (ST interval, PQ interval, and QS interval), peak (minimum and maximum peaks of P, Q, R, S, and T), and angle. This method is a type Of machine learning where features are extracted directly based on the learning performed. Israel extracted 15 time-interval features by determining the maximum local value based on P, R, and S peaks, tracking the slope, and identifying the position of the minimum curve radius for personal identification using ECG. Jahiruzzaman used the continuous wavelet transform (CWT) for extracting features as a representation of the time domain used for signal processing tasks such as image compression and pattern recognition. Personal by applying the encryption technology to ECG signals through CWT. Zhao used ensemble empirical mode decomposition (EEMD) and Welch spectrum analysis to extract intrinsic mode function (IMF) spectral features for obtaining the morphological and spectral information of signals. However, handcrafted feature extraction methods entail problems because the detection of peaks causes high variability in signals. Furthermore, these methods display reduced performance while removing noises or extracting features. Consequently, the emergence of deep learning resulted in the increased use of long short-term memory (LSTM). LSTM improves the performance of time-series and convolutional neural networks (CNNs), which display remarkable, image classification performance. Deep learning extracts features through learning. Therefore, features need not be extracted directly as in handcrafted feature extraction methods. Non-handcrafted fiducially-based methods need to detect the R-peak for the signal division because characteristic points are not used based on the overall form of ECG signals. For personal identification based on ECG, Labati proposed CNN-based deep-ECG using the PTB database. They performed pre-processing, CNN feature extraction, and identification in that order. A notch filter, infinite impulse response (IIR) filter, and third-order high-pass filter are used in the pre-processing step. The CNN consisting of six convolutional layers, a dropout layer, a fully-connected layer, and a softmax layer performed personal identification. Abdeldayem proposed five approaches for personal

identification using ECG. First, signals are distinguished using the cyclic characteristics of ECG signals. Second, the method of dividing and using the blind with constant duration of each segment, which is the period fixed to the ECG signal, can lower the complex calculation and improve the performance. This approach should incorporate the cyclic characteristic of the ECG mentioned above. Third, a noise removal step is not applied because the noise is not applied with a circulatory stop. Fourth, a 2D-CNN is used by transforming it into a power spectral density, which is the frequency domain of signals. Finally, eight open databases are combined into a database. Ciocoiu removed noises through a band-pass filter in a preprocessing step for ECG signals and divided the cycle by a constant time with respect to the R-peak. After transforming the data into images using four types of spatial representation (namely, CWT, Gramian angular field (GAF), phase-space trajectories, and recurrence plots), a CNN consisting of three convolutional layers, activation function ReLU, a max pooling layer, a fully-connected layer, and a softmax layer was applied for a comparative analysis of the accuracy and equal error rate (EER) of ECG-based biometric recognition. Y. H. Byeon used a CNN model of transfer learning for various time–frequency representations to examine the performance of ECG biometric Recognition. Four transfer learning models using MFCC, spectrogram, log spectrogram, mel spectrogram, and scalogram were employed as a time–frequency representation method. G. H. Choi proposed a personal identification method where multidimensional features are extracted by adjusting the bi-cubic 2D size for maintaining the data values and converting the ECG signals into a spectrogram. Noises are removed through preprocessing, and the signals are divided into a cycle consisting of a P wave, QRS complex wave, and T wave for personal identification. The divided signals are converted into a spectrogram to reduce the image size by 1/2 and 1/4 for identifying users. D. Jyotishi proposed a method of classification by adding the output of LSTM cells for personal identification using ECG signals. In the proposed model, the variations in bit could be observed because the signals were divided into smaller units considering the fluctuations in bit. Moreover, personal identification was performed according to various window lengths. J. S. Kim proposed a personal identification method based on a 2D coupling image using the cycle information of ECG signals. A 2D coupling image uses a CNN consisting of 12 convolutional layers and six max pooling layers for ECG-based user recognition. M. Hammad proposed an end-to-end deep neural network (DNN) for ECG-based authentication. The first model was designed as a 1D-CNN consisting of four convolutional layers, two max pooling layers, two fully-connected layers, and one max pooling layer. The convolution product of a CNN can efficiently extract morphological features from time-series or image identification was performed on the MIT/BIH arrhythmia database using ID matching

The second model was designed as ResNet-Attention. It combines the output of the first class consisting of two convolutional layers, a normalization layer, a ReLU layer, and a dropout layer, with that of the second class consisting of two normalization layers, two ReLU layers, two dropout layers, and two convolutional layers to be used as the input of Attention. Attention inspects the user authentication performance through two dense layers, a ReLU layer and a softmax layer. In this study, personal identification is carried

out based on the ensemble of LSTM and CNN by using ECG. The CU-ECG database constructed at Chosun University is used in the study. Non-handcrafted fiducial-based methods involve the detection of the R-peak of signals and division at certain intervals. Furthermore, short-time Fourier transform (STFT), scalogram, Fourier synchrosqueezed transform (FSST), and wavelet synchrosqueezed transform (WSST) are used as time–frequency representations to convert these into images. For classifying 1D time-series signals, LSTM as well as GoogleNet, VGG-19, and ResNet-101 (which are CNN transfer learning models with remarkable image classification performance) are used to inspect the performance. In addition, the improvement in performance is examined by the ensemble method.

4.1 LSTM

LSTM is the architecture of a recurrent neural network (RNN). An RNN is a neural network having a recurrent structure of output and input. Figure 1 shows the basic structure of an RNN. When a sequence with a large number of time steps is used in an RNN, the initial values decrease by the chain rule. This is because the values between $\square 1$ and 1

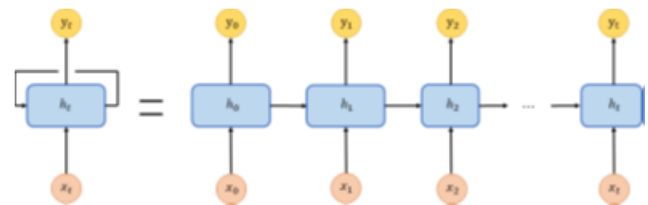


Figure 13: Structure of RNN

are multiplied by the hyperbolic tangent function (\tanh) in the back propagation through time (BPTT) used for training as the network becomes deeper. Therefore, an RNN involves the problem of information loss because the initial input data do not influence the output results owing to the vanishing gradient problem.

An LSTM with a structure more complex than that of an RNN was proposed to solve the long-term dependency problem of an RNN. An LSTM consists of an input gate, forget gate, and output gate for preventing information loss. The sigmoid activation function outputs a value between zero and one to determine the amount of information based on the output value. Thus, it can add or remove the information of the cell state. The sigmoid and hyperbolic tangent functions are used as the activation functions of an LSTM. The input gate determines whether new information is saved in the cell state, whereas the forget gate determines whether past information is deleted from the cell state. Meanwhile, the output gate determines which information is to be output from the cell state. Figure 2 shows the structure of an LSTM

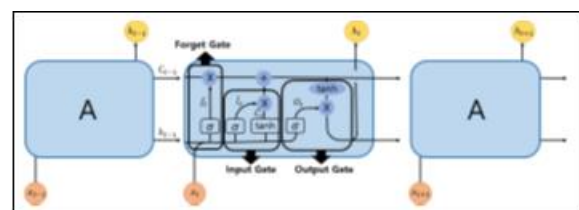


Figure 14: Structure of LSTM

Equations (1)–(6) show the process of updating the cell state and the output values of each gate by using the LSTM calculations. h_{t-1} represents the previous state, x_t represents the cell input, and h_t represents the cell output. w and a represent the weight and bias, respectively.

4.2 CNN

Deep learning is a type of machine learning technique. It is a neural network designed to have a structure similar to that of a neuron of the human brain. It refers to a DNN consisting of multiple layers including input layer, hidden layer, and output layer. A DNN has at least two hidden layers. Earlier, shallow neural networks could not perform complex computations and vanishing gradient or over fitting occurred during the learning process. However, a DNN enables learning and yields high performance by solving similar problems.

A CNN is a type of deep learning architecture. It is most widely used for image and time-series data. A CNN is a highly appropriate architecture for analysing and processing 2D data because features are extracted from input data through convolution products. A CNN

Consists of a repeating convolutional layer, ReLU activation function layer, and pooling layer.

$$f_c = \sigma(w_f \cdot [h_{t-1}, x_t] + a_f) \tag{1}$$

$$i_c = \sigma(w_i \cdot [h_{t-1}, x_t] + a_i) \tag{2}$$

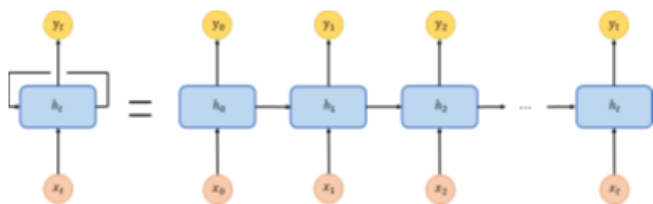
$$c_t = \tanh(w_c \cdot [h_{t-1}, x_t] + a_c) \tag{3}$$

$$\hat{c}_t = f_c \times C_{t-1} + i_c \times C_t \tag{4}$$

$$o_t = \sigma(w_o \cdot [h_{t-1}, x_t] + a_o) \tag{5}$$

$$h_t = o_t \times \tanh(C_t) \tag{6}$$

A convolutional layer is for extracting features from input data through the convolution product. The computation function outputs values by adding and multiplying each element of a moving filter and the filter size image. Padding is the process of filling the surrounding values of input data with zero. It prevents the size of input data from decreasing by the convolution product computation for adjusting the output size. Stride is the process of performing the convolution product when the filter moves according to the stride value by the interval in which the filter is applied to the input image. An activation function is a non-linear function positioned between convolutional layers and pooling layer. It includes sigmoid, ReLU, step function, hyperbolic tangent, and softmax functions. ReLU is mostly used as an activation function. The ReLU function is expressed as zero and one. Herein, a negative value is output as zero, and any value higher than zero would be output directly as the input. Equation (7) presents the ReLU function.



$$R_x = \max(0, x), R_x = \begin{cases} 0 & (x < 0) \\ x & (x \geq 0) \end{cases}$$

A pooling layer reduces the dimensions while maintaining important features of an image. Pooling layers are of several types such as max pooling, average pooling, and L2-norm pooling. A max pooling layer is most commonly used where the maximum values of each domain are expressed for the target domain. A fully-connected layer is used for classifying images in 1D form. In this layer, a neuron of a previous layer is connected with one of the next layer. A softmax layer shows the final classification result as a probability where the sum of output values is always one. Accordingly, a CNN demonstrates remarkable performance in image classification by adding a convolutional layer and pooling layer to a conventional neural network.

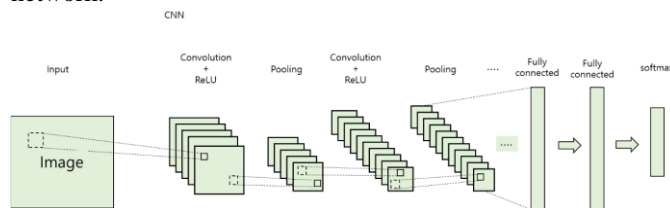


Figure 15: Structure of CNN

4.3 Proposed Personal Identification Based on Intelligent Micro Fluid Chip

An LSTM neural network is used for identifying the sequential information to analyse 1D time-series or sequence signals. An LSTM consists of a sequence input layer for entering time-series or sequence data, an LSTM layer for training long-term dependency between time-steps of a sequence, a fully-connected layer for classifying class labels, a softmax layer, and a classification layer. Because the classification accuracy improves as units consisting of the numbers of hidden layers and three cells increase, the deep structure of an LSTM neural network can be expanded by adding LSTM layers. Figures 4 and 5 show examples of one LSTM layer and two LSTM layers, respectively. Appl. Sci. 2021, 11, x FOR PEER REVIEW 6 of 20 A convolutional features from input data through the convolution product. The computation function outputs values by adding and multiplying each element of a moving filter and the filter size image. Padding is the process of filling the surrounding values of input data with zero. It prevents the size of input data from decreasing by the convolution product computation for adjusting the output size. Stride is the process of performing the convolution product when the filter moves according to the stride value by the interval in which the filter is applied to the input image. An activation function is a non-linear function positioned between convolutional layers and pooling layer. It includes sigmoid, ReLU, step function, hyperbolic tangent, and softmax functions.

ReLU is mostly used as an activation function. The ReLU function is expressed as zero and one. Herein, a negative value is output as zero, and any value higher than zero would be output directly as the input. Equation (7) presents the ReLU function.

$$R_x = \max(0, x), \quad R_x = \{0 \ (x < 0) \ x \ (x \geq 0)\} \quad (7)$$

A pooling layer reduces the dimensions while maintaining important features of an image. Pooling layers are of several types such as max pooling, average pooling, and L2- norm pooling. A max pooling layer is most commonly used where the maximum values of each domain are expressed for the target domain. A fully-connected layer is used for classifying images in 1D form. In this layer, a neuron of a previous layer is connected with one of the next layer. A softmax layer shows the final classification result as a probability where the sum of output values is always one. Accordingly, a CNN demonstrates remarkable performance in image classification by adding a convolutional layer and pooling layer to a conventional neural network.



Figure 16: Future Human's Universal Code

4.4. Time-Frequency Transform

Because physiological signals are affected considerably by noises, the data are transformed into the time-frequency domain and expressed in a 2D image for signal analysis.

ECG signals use 2D images transformed by STFT, scalogram, and FSST through a time-frequency transform. The images expressed through a time-frequency transform are classified with a CNN, which displays remarkable image-classification performance.

4.5 STFT

A Fourier transform is a frequency representation where time-series signals are decomposed into a frequency. Frequencies observed in signals can be analysed. However, the variations over time are not considered. The conventional Fourier transform is insufficient to analyse images because the position of each frequency with respect to time cannot be identified [23]. Therefore, STFT and DTFT have been researched to overcome these drawbacks.

STFT divides a long signal that varies over time into shorter lengths to apply the Fourier transform. The presence of a specific frequency at a specific time can be identified when signals are divided into shorter time-lengths, and whether a specific frequency is present within a specific time can be identified when signals are divided into longer time-lengths. That is, a smaller window width is more advantageous for time resolution, whereas a larger one is more advantageous for frequency resolution. Figure 6 shows the image of the time-frequency representation by STFT.

Equation (8) shows the process of dividing the signals of STFT, which is expressed in terms of signals and a moving window function. Equation (9) is the Fourier transform computation of STFT in terms of the signal $x(t)$ and window function $w(t)$ with respect to time t .

$$x(a, t) = x(t) \times w(t - a) \quad (8)$$

$$x(a, v) = \int_{-\infty}^{\infty} x(t)w(t - a)e^{-it} \quad (9)$$

4.6. Scalogram

A scalogram is the absolute value of the continuous wavelet transform (CWT) with respect to signals. A wavelet is explained below because the CWT is computed for expressing a scalogram. STFT complements the drawback of the conventional Fourier transform (namely that whereas detailed information on either of time and frequency according to the window length can be obtained, it is difficult to obtain the information of both time and frequency owing to a fixed window length). A wavelet transform has been recommended to overcome this limitation of STFT. In addition, wavelet transform can be time, and frequency can be simultaneously identified in the CWT domain. A wavelet transform increases the time resolution in the signals of the high-frequency domain while lowering the frequency resolution and increases the frequency resolution in the signals of the low-frequency domain while decreasing the time resolution. Thereby, both time and frequency information can be identified simultaneously. Thus, it is efficient for analysing discontinuous signals. The conventional Fourier transform uses an infinite sine function in the time domain, whereas a wavelet transform uses a mother wavelet function that is limited in the time domain. This enables signals to be analysed in time and frequency domains through the scaling and shifting of signals [24]. Equation (10) shows the wavelet transforms (CWT). m and n mean resizing the mother wavelet and shifting of the mother wavelet, respectively. $h(t)$ is the input signal, and ψ is the mother wavelet.

$$G(m, n) = \frac{1}{\sqrt{m}} \int_{-\infty}^{\infty} h(t)\psi\left(\frac{t-n}{m}\right) dt \quad (10)$$

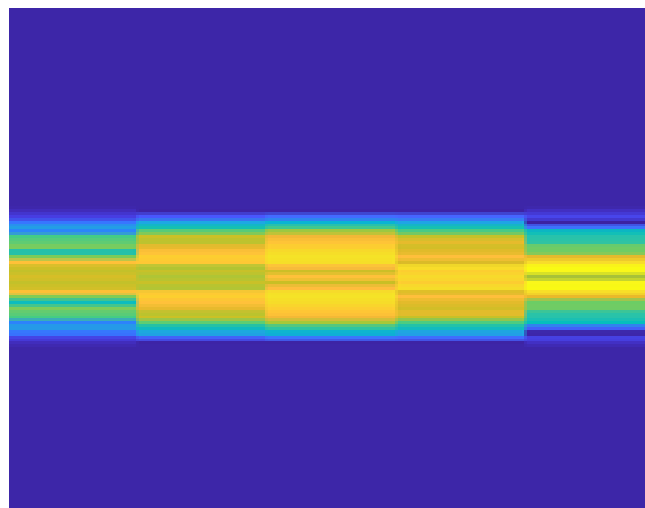


Figure 17: Time-frequency representation by STFT

There are various types of mother wavelets, and different analysis results are expressed depending on the wavelet type. Therefore, an appropriate type of a mother wavelet must be used for each analysis type. The mother wavelets used for the CWT include Morse, Morlet, and bump wavelets. Morse wavelets are suitable for analysing signals having time, frequency, and amplitude. Equation (11) represents the Fourier transform of the Morse

Wavelet. Here, $P(\omega)$ is the unit time; $h_{T,\mu}$ is the normalization constant; and T and μ are the products of parameters for representing the symmetry of the Morse wavelet, time, and bandwidth. μ is a damping or compressing parameter rather than the product of time and bandwidth. Here, Equation (12) shows the Morse wavelet equation in terms of the parameterization of T and μ . Two parameters can be adjusted as required to represent the Morse wavelet. T is the product of time and bandwidth and is proportional to the wavelet duration, which varies over time. In addition, duration is the frequency at which the maximum peak frequency is positioned in the centre of the window. Here, Equation (13) expresses the maximum peak frequency. μ controls the symmetry of a wavelet, which varies over time.

$$\psi_{T,\mu}(\omega) = P(\omega)h_{T,\mu}\omega^{\frac{T}{\mu}}e^{-\omega\mu} \tag{11}$$

$$\psi_{\alpha,\mu}(\omega) = P(x)h_{\alpha,\mu}\omega^{\alpha}e^{-\omega\mu} \tag{12}$$

$$\left(\frac{T^2}{\mu}\right)^{\frac{1}{\mu}} \tag{13}$$

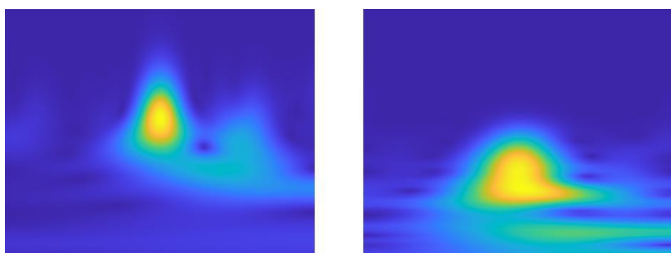


Figure 18: Morse wavelet according to T2. (a) T2 = 10. (b) T2 = 60.

4.7. 2D Transform-Based CNN

Images that are represented through time–frequency transforms such as STFT, scalogram, FSST, and WSST use a CNN, which is highly capable of image classification. A Appl. Sci. 2022, 12, 2692 11 of 19 CNN can be designed directly to examine its performance. Alternatively, transfer learning including a CNN model can be used to inspect the performance. A substantial data is required for training a CNN-based deep learning model. In addition, the training time is long for a complex model, where the number of layers and hyperparameters need to be adjusted according to data. Therefore, transfer learning (a CNN model) is used.

Transfer learning such as AlexNet, Google Net, VGG, ResNet, and SqueezeNet involves training new data using a previously developed model and is applicable for cases with a marginal amount of data. GoogleNet, VGG-19, and ResNet-101 are used as a 2D transform based CNN. As shown in Figure 10, Google Net is a DNN with 22 trainable layers and 9 inception models. Furthermore, Google Net consists of parallel

convolution filters without puts connected from the inception modules. Figure 11 shows the inception module with four types of operations: 1 1 convolution product, 1 1 convolution product + 3 3 convolution product, 1 1 convolution product + 5 5 convolution product, and 3 3 max pooling + 1 1 convolution product. These operations are used to reduce the Number of operations required by decreasing the number of parameters and adjusting the number of channels. The loss values generated during the training are added to prevent the vanishing gradient problem in DNNs such as Google Net. Figure 9. Time–frequency representation by WSST. 3.3. 2D Transform-Based CNN

Images that are represented through time–frequency transforms such as STFT, scalogram, FSST, and WSST use a CNN, which is highly capable of image classification. A CNN can be designed directly to examine its performance. Alternatively, transfer learning including a CNN model can be used to inspect the performance. A substantial amount of Therefore, transfer learning (a CNN model) is used. amount of data. Google Net, VGG-19, and ResNet-101 are used as a 2D transform- based CNN. As shown in Figure 10, Google Net is a DNN with 22 trainable layers and 9 inception models. Furthermore, Google Net consists of parallel convolution filters with outputs connected from the inception modules. Figure 11 shows the inception module with four types of operations: 1 × 1 convolution product, 1 × 1 convolution product + 3 × 3 convolution product, 1 × 1 convolution product + 5 × 5 convolution product, and 3 × 3 max pooling + 1 × 1 convolution product. These operations are used to reduce the number of operations required by decreasing the number of parameters and adjusting the number of channels. The loss values generated during the training are added to prevent the vanishing gradient problem in DNNs such as Google

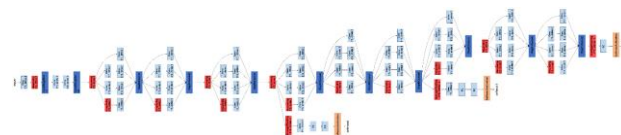


Figure 19: Structure of Google net

4.8. Proposed Intelligent Micro Fluid Chip Personal Identification

The performance of various models can be compared by training these and selecting those with a higher performance. However, when an individual model with remarkable performance is used, the performance improvement in other models can be omitted. Thus, the performance can be improved further by combining different models. An ensemble is a technique for improving performance by combining different models. It can demonstrate performance higher than that of the individual models. Computation, representation, and statistics can be improved by deep learning models and ensembles. An ensemble uses the voting method, average, maximum, and multiplication for the output values of each model to predict the final results.

In this study, the deep learning models LSTM and 2D-CNN are combined for personal identification. The numbers of hidden layers and units are increased to enhance the classification accuracy, and LSTM layers are added to deepen the LSTM. Furthermore, 1D ECG signals are transformed to

2D data by using time–frequency representation methods. Three pre-trained CNN models (namely, Google Net, VGG-19, and ResNet-101) are used. An ensemble method for combining the output values of two models is used to enhance the performance of an individual model. An ensemble performs personal identification by determining the final prediction results using the output values of each model for an identical input. Personal identification using ECG can be divided into three steps: signal pre-processing, feature extraction and learning, and personal identification.

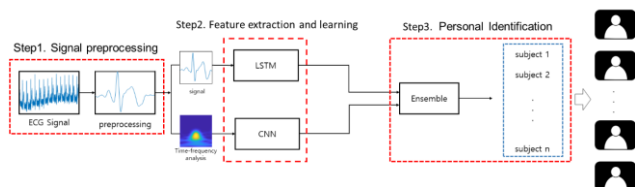


Figure 20: Flowchart of proposed Intelligent Micro Fluid Chip personal identification.

In the first step of signal pre-processing, noises need to be removed for maintaining the shape of ECG signals. This is because the signals can be distorted by various noises during measurement. In an ECG, breathing, friction between skin and electrode, noise Figure 15. Flowchart of proposed ensemble-based personal identification. This is the In an ECG, breathing, friction between skin and electrode, noise from muscles, and noise from contact between electrode and power line are included during measurements. In this paper, the noises of ECG signals were removed using a low-pass filter. A low pass filter is a filter that passes through a frequency signal below the cut-off frequency. This filter is used to remove high frequency components such as muscle noise, 60 Hz power line noise, and electrode contact noise and to soften the signal. These noises are removed through a low-pass filter as shown in Figure 16a, b. In Figure 16b, where noises have been removed, the baseline of the signal shifts above or below the x-axis of the signal. Fluctuations in the baseline are low-frequency vibrations generated by the breathing, sweat, or movement of a subject. These cause variations in the impedance between electrode and Skin. The baseline functions as the criteria for detecting characteristic points of ECG signals. Noises must be removed from the baseline because the morphological characteristics of ECG signals cannot be identified if the fluctuations in the baseline occur. the signals wherein the baseline has been calibrated with respect to zero, and Figure 16d shows the standardized signals.

ECG signals consist of a P wave, QRS complex wave, and T wave and include various cycles. Signals are divided to extract features of the ECG signals. , the R-peak is detected to divide the signal into a cycle with respect to the detected R-peak. The second feature extraction and learning stage is an important step that affects classification performance results. For this purpose, electrocardiogram data is applied to LSTM and 2D-CNN to extract and learn features, respectively. In order to use 2D-CNN, one-dimensional ECG signals need to be converted into two-dimensional images. Therefore, it is converted through four time-frequency representations such as STFT, Scalogram, FSST, and WSST, which are transformation methods, and a pre-trained model, Google Net, VGG- 19, ResNet-101 is used. The size of each image is reduced to 224 224, and Adam is applied as a learning method. The minimum

value of a loss function can be determined because Adam maintains both the moving average and momentum. The initial learning rate, epoch, and mini-batch size are set appropriately for the model to examine the personal identification performance. In the third step of personal identification, an ensemble that can display performance higher than that of an individual model is used by combining various models based on the personal identification results in the previous step of feature extraction and learning. An ensemble uses the multiplication of model outputs to determine the results. shows the flowchart of the proposed ensemble-based personal identification using STFT and Google Net among the four transform methods and three models used. Two databases classify the subjects by combining the output values of LSTM and CNN through pre-processing.

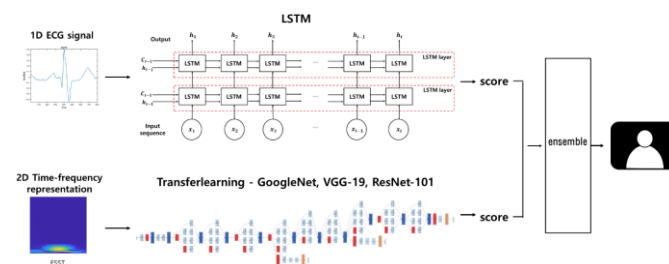


Figure 21: Flowchart of proposed ensemble-based personal identification

5. Conclusions

In this section, we cover some implementation comments, as well as the benefits and drawbacks of the methodologies under consideration, before presenting the data collection tools, datasets, and open-source evaluation tools.

1) Radar-Based HOD

We need to install unique gear inside earth for global level identify and detection when using radar-based approaches. Radar systems detect the presence, range, and direction of static or moving objects. This is achieved by sending out high-frequency electromagnetic field pulses (EMF). One critical issue for radar is its impact on human health, particularly in long-term use. As a result, radar-based occupancy detection systems should not be used for long-term indoor applications.

Radars commonly use RF frequencies ranging from 300 MHz to 15 GHz. The RF energy in this region of the electromagnetic spectrum is known to interact differently with the human body. RF fields below 10 GHz (to 1 MHz) enter exposed tissues and generate warmth due to energy absorption. The depth of penetration is affected by the frequency of the field, which is greater at lower frequencies. To assess how well RF fields are absorbed by tissues, a specific absorption rate (SAR) within a certain tissue mass is used. The SI unit for SAR is watts per kilogram (W/kg). SAR is a method for measuring RF field exposure in the 1 MHz to 10 GHz range. A SAR of at least 4W/kg is necessary to generate known unfavourable health effects in people exposed to RF fields in this frequency range. The skin surface absorbs RF fields over 10 GHz, with only a small amount of energy reaching deeper tissues. The fundamental dosimetric quantity for RF fields above 10 GHz is the field power density, defined in watts per square meter (W/m²) or, for weak fields, in milliwatts per square meter

(mW/m²) or micro-watts per square meter (W/m²). Eye cataracts and skin burns are just two of the negative health effects associated with exposure to RF fields above 10 GHz at power densities surpassing 1000W/m², according to analyze.

2) Wifi And Bluetooth

Bluetooth and BLE could only provide RSSI, as seen in Table 2, but WiFi access points could provide both RSSI and CSI. However, not all WiFi access points can generate channel state information. Active techniques, in which an extra device, such as a smartphone, is carried by the people in the room, usually involve some localization or tracking mixed with detection. The location of the user's mobile application can be determined based on the RSSI from multiple APs. Some of the studies that have been evaluated additionally monitor the number of connected devices to the APs or even assess the APs' energy usage, which is related to the number of connected devices. They attempt to establish a relationship between the number of connected devices and the number of people in the building or below ground level. Here, we concentrate on CSI data collection. One of the most frequently mentioned tools for gathering CSI is an open-source tool named "Atheros CSI". It allows for the extraction of detailed PHY wireless communication data such as the received packet payload and CSI (the time stamp, the RSSI of each antenna, the data rate, etc.). Atheros-CSI-Tool should theoretically support all Atheros 802.11n WiFi chipset types, including the tested Atheros AR9580, AR9590, AR9344, and QCA9558 because it is based on ath9k, an open source Linux kernel driver that supports Atheros 802.11n PCI/PCI-E chips. The sub-carrier for each CSI is a complex number ($a+bj$). The CSI of a packet sent across a 20MHz channel with M transmitting antennae, N receiving antennas, and $M \times N \times 114$ if the WiFi bandwidth is 40MHz is a sophisticated matrix of size $M \times N \times 56$. "Linux 802.11n CSI" [93] is known as another CSI collection tool. The Tool is built with free source Linux wireless drivers and Intel WiFi Wireless Link 5300 802.11n MIMO radios with custom firmware updates. This includes all of the programs and scripts needed to run experiments as well as read and analyze channel measurements. The IWL5300 provides 802.11n channel status data in the form of channel matrices for 30 subcarrier groups, or roughly one group for every two subcarriers at 20 MHz and one in every four at 40 MHz. Each channel matrix element is a complex number, with a signed 8-bit resolution in the real and imaginary portions. The signal strength and phase between a single transmit-receive antenna pair are provided.

FigureoScenes is a versatile and effective middleware for CSI-based WiFi sensing research. It assists researchers in overcoming two barriers to WiFi sensing research: a lack of measuring software functionality and a lack of hardware characteristics. FigureoScenes supports the most CSI-extractable devices, such as software-defined radio and commercial off-the-shelf (COTS) WiFi NICs. COTS NICS supported include the Intel WiFi 6E AX210 (AX210), Intel WiFi 6 AX200 (AX200), Qualcomm Atheros AR9300 (QCA9300), and Intel Wireless Link 5300. (IWL5300). All universal Software radio peripheral (USRP) versions, as well as additional SDR equipment, are supported. FigureoScenes is said to be the first and only publicly accessible platform that supports CSI extraction for 802.11ax-format frames utilizing ordinary WiFi hardware for the AX200 NIC. The platform supports CSI extraction for all formats (802.11a/g/n/ac/ax) and

bandwidths (20/40/80/160 MHz). Furthermore, FigureoScenes qualifies all overheard frames in monitor mode for CSI measurement, converting all surrounding WiFi devices into excitation signals for your sensing application.

There are many general-purpose devices, such as the Arduino, Raspberry Pi and USRP based on software-defined radio devices to provide RF architecture to design, prototype, and deploy wireless systems with custom signal processing.

It should be noted that recently produced WiFi routers include advanced capabilities for extracting CSI, which can be used for human occupancy detection and activity recognition. WiFi systems now support a variety of bands, including 2.4 GHz, 5 GHz, and 60 GHz, which provide faster data rates and more bandwidth for transmitting and receiving signals. Furthermore, modern WiFi routers include advanced antennas that use beam-steering and/or beam-forming technologies. These antennas can adjust the direction of the wireless signal dynamically to improve signal strength and reduce interference. This allows for the extraction of highly detailed CSI data, which can then be used to detect and track human presence and activity in indoor environments with high accuracy.

6. Acknowledgement

In this paper, we propose a Google net, Space shuttle, Radio signal, internal receiver without any tower and Human body system hosted on SIFT AI radio. Owing to the large bandwidth of UWB radio, our system can obtain richer motion features from RF signals compared to Wi-Fi-based solutions. To make our system work with resource-constrained edge device, a signal adapted convolutional neural network model is designed to extract features and classify activities without third party or external service. The system is going to evaluate in multiple real-life environments and comprehensive experiments demonstrate that main approach can obtain a precision of 99.9% and a recall of 99.5%. We believe the proposed methods can benefit a large range of other sensing applications. In the future, we plan to implement this system for reduce list of identification.

Numerous factors, including increasing Crime, Unidentified missing information, Human behind memories. We can help ourselves by reducing

No more

- Adhar card
- Green card
- Tazkira
- Estonia
- eHerkenning
- Documento
- Nacional de Identidad
- Şəxsiyyət vəsiqəsi
- Central Popular Registration National identity card
- Belarus national identity card
- Personalausweis Bhutan citizenship card
- Omang
- Cédula de Identidade
- Resident Identity Card
- National ID card Ghana

- Card Greek identity card
- Carte nationale d'identité
- Guyana national identity card
- Hong Kong Identity Card
- Iraq National Card
- Teudat Zehut
- Carte Nationale d'Identité
- Kuwaiti identity card
- MyKad Computerised National Identity Card
- ATM card
- Staff ID card
- Student ID card
- Passport
- Visa
- Birth certificate
- Education certificate
- Biometric
- Scanner machine
- No paper work
- No more spelling mistake
- No more long line in queue

A Single ID card will cover human history and saving in to unidentified location with high level security, private security.

The particular device will identify his stored data's.

Example

- Traffic police follow his card, he get His device contains information about transportation.
- The student data will be received by the education department. The organization will acquire employee data.
- To cross country line, an immigration officer will obtain information regarding authorization to work or visit.
- Cardholders' health information will be available to doctors.
- He/She can fly or move with a single card around world with work permit.
- This ID card will not destroy or scratch.
- Any one missed his card, within in 24 hours he gets back.
- This card network linked with his in build Coccyx IMFC.
- Coccyx IMFC linked with his brain
- His brain linked with space shuttle.

The person going to control by universal network.

We can identify within micro seconds where they are.

Under control By Y2C

- Zero Crime
- Zero Missing information
- Un identified human bodies
- Flight hijack
- Crossing borders
- Border security force
- Machinery usage

Earth will be back to its original axis.

Project cost: Half of Reserve bank of India stock Money.

We save 500 times of project cost every 20 years.

Except if coccyx never decayed the IMFC won't harm as long as he can remember.

A Solitary card with Universal code.

57321906071998560052

References

- [1] Priya M.S in honor of her Intelligence work on Multilevel Image Thresholding using OTSU's Algorithm in Image Segmentation International Journal of Scientific & Engineering Research Volume 8, Issue 5, May-2017
- [2] Gabriela Slizewska Graduate Student · University of Pittsburgh Pittsburgh, Pennsylvania, United States. Bermúdez, Jos, Luis; Marcel, Anthony & Eilan, Naomi eds. (1995), *The Body and the Self* (Cambridge, MA & London: The MIT Press)
- [3] Blakemore, Colin & Greenfield, Susan eds. (1987), *Mind waves* (Oxford: Blackwell)
- [4] Jeong, D. Artificial intelligence security threat, crime, and forensics: Taxonomy and open issues. *IEEE Access* 2020, 8, 184560–184574. [Google Scholar] [CrossRef]
- [5] Kim, J.; Rhee, P. Image recognition based on adaptive deep learning. *Inst. Internet Broadcast. Commun.* 2018, 18, 113–117. [Google Scholar]
- [6] Lu, L.; Mao, J.; Wang, W.; Ding, G.; Zhang, Z. A study of personal recognition method based on emg signal. *IEEE Trans. Biomed. Circuits Syst.* 2020, 14, 681–691. [Google Scholar] [CrossRef] [PubMed]
- [7] Rabuzin, K.; Baca, M.; Sajko, M. E-learning: Biometrics as a security factor. In *Proceedings of the International Multi-Conference on Computing in the Global Information Technology*, Bucharest, Romania, 1–3 August 2006; p. 64. [Google Scholar]
- [8] Barros, A.; Rosário, D.; Resque, P.; Cerqueira, E. Heart of IoT: ECG as biometric sign for authentication and identification. In *Proceedings of the 15th International Wireless Communications & Mobile Computing Conference (IWCMC)*, Tangier, Morocco, 24–28 June 2019; pp. 307–312. [Google Scholar]
- [9] Jiang, X.; Xu, K.; Liu, X.; Dai, C.; Clifton, A.D.; Clancy, A.E.; Akay, M.; Chen, W. Cancelable HD-sEMG-based biometrics for cross-application discrepant personal identification. *IEEE J. Biomed. Health Inform.* 2021, 25, 1070–1079. [Google Scholar] [CrossRef]
- [10] Biel, L.; Pettersson, O.; Philipson, L.; Wide, P. ECG analysis: A new approach in human identification. *IEEE Trans. Instrum. Meas.* 2001, 50, 808–812. [Google Scholar] [CrossRef] [Green Version]
- [11] Ingale, M.; Cordeiro, R.; Thentu, S.; Park, Y.; Karimian, N. ECG biometric authentication: A comparative analysis. *IEEE Access* 2020, 8, 117853–117866. [Google Scholar] [CrossRef]
- [12] Zhang, Q.; Zhou, D.; Zeng, X. HeartID: A multiresolution convolutional neural network for ECG-Based biometric human identification in smart health

- applications. IEEE Access 2017, 5, 11805–11816.
[Google Scholar] [CrossRef]
- [13] Israel, S.A.; Irvine, J.M.; Cheng, A.; Wiederhold, M.D.; Wiederhold, B.K. ECG to identify individuals. *Pattern Recognit.* 2005, 38, 113–142.
[Google Scholar] [CrossRef]
- [14] Jahiruzzaman, M.; Hossain, A.B.M.A. ECG based biometric human identification using chaotic encryption. In *Proceedings of the International Conference on Electrical Engineering and Information Communication Technology (ICEEICT)*, Savar, Bangladesh, 21–23 May 2015; pp. 1–5. [Google Scholar]
- [15] Zhao, Z.; Yang, L.; Chen, D.; Luo, Y. A human ECG identification system based on ensemble empirical mode decomposition. *Sensors* 2013, 13, 6832–6864.
[Google Scholar] [CrossRef] [Green Version]
- [16] Wiclaw, L.; Khoma, Y.; Fałat, P.; Sabodashko, D.; Herasymenko, V. Biometric identification from raw ECG signal using deep learning techniques. In *Proceedings of the 9th IEEE International Conference on Intelligent Data Acquisition and Advanced Computing Systems: Technology and Applications (IDAACS)*, Bucharest, Romania, 21–23 September 2017; pp. 129–133. [Google Scholar]
- [17] Labati, R.D.; Muñoz, E.; Piuri, V.; Sassi, R.; Scotti, F. Deep-ECG: Convolutional neural networks for ECG biometric recognition. *Pattern Recognit. Lett.* 2019, 126, 78–85. [Google Scholar] [CrossRef]
- [18] Abhijit Dasgupta a, Rajat K. De b Department of Structural Biology, St. Jude Children's Research Hospital, Memphis, TN, United States
- [19] T. Neil Davis, 2156 Koyukuk Drive, University of Alaska Fairbanks, Fairbanks, AK 99775
- [20] Jin-A Lee and Keun-Chang Kwak Department of Electronic Engineering IT-Bio Convergence System, Chosun University, Gwangju 61452, Korea;
- [21] 45 SPW HB S-100/KHB 1700.7, Space Transportation System Payload Ground Safety Handbook.
- [22] SPW HB S-100/KHB 1700.7, Space Transportation System Payload Ground Safety Handbook.
- [23] SPW HB S-100/KHB 1700.7, Space Transportation System Payload Ground Safety Handbook.
- [24] World Scientific Europe, Connecting Great Minds.
- [25] Ismail al-Jazari. The Book of Knowledge of Ingenious Mechanical Devices. 'Book in knowledge of engineering tricks' in 1206. Mesopotamia, Turkey.
- [26] The Coccyx Miracle in Islam and Science.
- [27] Google Images.
Indian Sociology.